# NJC

## Accepted Manuscript

This is an *Accepted Manuscript*, which has been through the Royal Society of Chemistry peer review process and has been accepted for publication.

*Accepted Manuscripts* are published online shortly after acceptance, before technical editing, formatting and proof reading. Using this free service, authors can make their results available to the community, in citable form, before we publish the edited article. We will replace this *Accepted Manuscript* with the edited and formatted *Advance Article* as soon as it is available.

You can find more information about *Accepted Manuscripts* in the **Information for Authors**.

Please note that technical editing may introduce minor changes to the text and/or graphics, which may alter content. The journal's standard **Terms & Conditions** and the **Ethical guidelines** still apply. In no event shall the Royal Society of Chemistry be held responsible for any errors or omissions in this *Accepted Manuscript* or any consequences arising from the use of any information it contains.

# New Journal of Chemistry

**PAPER**

## Fluorescent silica nanoparticles modified chemically with terbium complexes as potential bioimaging probes: Their fluorescent and colloidal properties in water

Yoshio Nakahara,[a] Yoichi Tatsumi,[a] Ikuko Akimoto,[a] Shusuke Osaki,[b] Motomichi Doi[c] and Keiichi Kimura[a]*

It generally requires a complicated reaction protocol for the synthesis of silylated fluorescent lanthanide complexes. In this study, a silylated terbium complex was prepared with a very simple procedure through a formation of a Schiff base between a terbium complex bearing a formyl group and 3-aminopropyltriethoxysilane. Using the silylated terbium complex, highly fluorescent silica nanoparticles modified chemically with terbium complexes (**Tb-SNPs**) were efficiently synthesized by a reverse micelle method with Triton X-100 as a surfactant in cyclohexane. Fluorescent properties of **Tb-SNPs** were remarkably improved by photostability, pH dependence and fluorescence lifetime, compared to free terbium complexes. Also, **Tb-SNPs** hardly aggregated under aqueous conditions with different salt concentrations and pHs. From these results, it was found that **Tb-SNPs** are applicable under physiological aqueous conditions. Furthermore, as an application model, **Tb-SNPs** were used as the fluorescent label for the imaging of African green monkey kidney cells.

## Introduction

Lanthanide complexes are expected as fluorescent probes for biological assay because of their characteristic fluorescent properties such as multiple sharp emission bands (< 10 nm) and large Stoke's shifts (> 150 nm).[1-3] In addition, their long-lived fluorescence lifetime is applicable for time-resolved luminescence, which allows the elimination of the background interference originating from autofluorescence and excitation light scattering.[4-6] For these advantages over traditional probes, some conjugate fluorescent lanthanide probes to antibodies, oligonucleotides and proteins have been developed so far.[7-9]

Fluorescent probes must be soluble, stable and sufficiently bright in water for practical biological applications.[10] However, it is generally known that the fluorescent property of lanthanide complexes is significantly deteriorated based on the quenching by water molecules.[11,12] Therefore, much efforts to enhance aqueous fluorescent properties of lanthanide complexes have been attempted for the application in water.[13-15] Among them, organic/inorganic nanoparticles containing thousands of fluorescent lanthanide complexes have been well established for bioanalysis in order to improve the brightness and water solubility of their fluorescent probes. Polystyrene nanoparticles doped physically with lanthanide complexes were explored as ultrasensitive fluorescent labels, but this type of polystyrene nanoparticles suffered from the risk of complexes dissolving out from the nanoparticle.[6] Recently, silica-based nanoparticles containing fluorescent lanthanide complexes have been developed in the biological field because the silica shell provides high dispersibility in water, possible surface functionalization and biocompatibility.[16-19] Additionally, silylated fluorescent probes can be covalently linked to silica nanoparticles, which solves the leaking problem.[20] Fluorescent lanthanide complexes have been often connected with organosilane species, and they were introduced chemically into silica materials by a conventional sol-gel process. Very interestingly, photochemical stability of fluorescent lanthanide complexes was remarkably improved by the immobilization into silica matrix.[21,22] On the other hand, very few silylated fluorescent lanthanide complexes have been developed because their syntheses were quite complicated.[18,23-25]

In this study, we designed and prepared novel fluorescent nanoparticles modified chemically with terbium complexes (**Tb-SNPs**), which are schematically illustrated in Fig. 1. In the complex, a formyl group works as an antenna ligand, which brings about the efficient intramolecular energy transfer from a light absorption moiety to a central lanthanide ion. A silylated terbium complex was prepared with a very simple procedure through a formation of a Schiff base between a terbium complex bearing a formyl group and 3-aminotriethoxysilane (APTES) because Schiff bases can be obtained in excellent purity.[26,27] Then, its sol-gel copolymerization with tetraethoxysilane (TEOS) was carried out in a reverse micelle method using Triton X-100 as a surfactant in cyclohexane. After the elaborate characterization of **Tb-SNPs**, fluorescent properties of covalently linked terbium complexes in silica nanoparticles were evaluated in parallel with that in solution with respect to photochemical stability, pH stability and fluorescence lifetime. Finally, as an application model, the

imaging of African green monkey kidney cells was performed using **Tb-SNPs** as the fluorescent label.
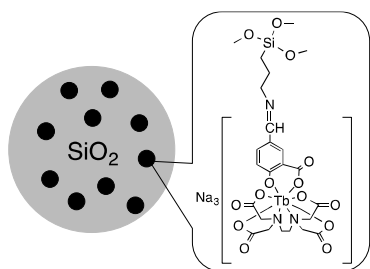


**Fig. 1** Schematic illustration of **Tb-SNPs**.

## Experimental

### Chemicals

Terbium acetate tetrahydrate, 5-formylsalicylic acid (FSA), cyclohexane, 1-hexanol, acetic acid, sodium hydroxide and sodium chloride were purchased from Wako Pure Chemical Industries and used without further purification. Tetraethoxysilane (TEOS) and 3-aminopropyltriethoxysilane (APTES) were purchased from Sigma-Aldrich Japan K. K. and used without further purification. Triton X-100 and disodium ethylenediamine tetraacetate dihydrate (EDTA) were purchased from Kishida Chemical and Katayama Chemical Industries, respectively and used without further purification. Deionized water (resistivity: 18 MΩ cm) was prepared using a Milli-Q system.

### Instrumentation

Centrifugation was performed using a himac CS100GX2 with S50A rotor (Hitachi-koki) at 40,000 rpm for 8 min. Elemental analysis was carried out using a JM10 Micro Corder (J-Science). The UV-vis spectra were measured with a V-550 UV/VIS spectrophotometer (Jasco) at 25°C and quarts cells of 1-cm optical path length. The scanning electron microscope (SEM) studies were carried out with a JSM-6390 microscope (JEOL). The size distribution and $\zeta$ potential of nanoparticles were recorded at 25°C using a particle size analyzer (Otsuka Electronics, ELS Z). The size distribution was evaluated by dynamic light scattering (DLS). The inductively coupled mass spectrometry (ICP-MS) was performed using an Agilent 7500cx (Agilent) for determining the concentration of terbium ion. The fluorescence spectra were recorded at 25°C with a spectrofluorophotometer (Shimadzu, RF-5300PC). The UV light was irradiated to a quartz cell containing a sample solution through a color filter (Toshiba Glass, UV-D36B) with a Xe lamp (Hamamatsu Photonics, LC5). Decay curves were measured by a digital oscilloscope (Tektronix, TDS3032) with a photomultiplier (Hamamatsu Photonics, R3896) attached to a monochromator (Acton, 300i), where spectral resolution was 4 nm. Fluorescence spectra were detected by an Intensified CCD (Roper, PI-MAX). Photoexcitation was performed by nanosecond pulses from a nitrogen gas laser (Horiba). Power of laser pulses was < 10 μJ cm$^{-2}$.

### Synthesis

The synthesis of the terbium complex bearing a formyl group (**EDTA-FSA-Tb complex**) was carried out according to the previous reported method.[28] An aqueous solution (8.0 mL) of EDTA (0.47 g, 1.3 mmol) and sodium hydroxide (0.10 g, 2.5 mmol) was added to an aqueous solution (10 mL) of terbium acetate tetrahydrate (0.51 g, 1.3 mmol), and the resulting mixture was stirred for 1 h at 60°C. After then, an aqueous solution (7.5 mL) of FSA (0.21 g, 1.3 mmol) and sodium hydroxide (0.10 g, 2.5 mmol) was added to the mixture, and the resulting mixture was stirred for 1 h at 60°C. After the reaction completed, the solvent was evaporated. The residue was purified by reprecipitation from water into warmed ethanol at 60°C: white solid, yield 89%. Anal. calcd for $C_{18}H_{16}N_2O_{12}Na_3Tb\cdot4H_2O$: C, 28.73; H, 3.19; N, 3.72%. Found: C, 28.70; H, 3.39; N, 4.09%. The quantum yield of **EDTA-FSA-Tb complex** was determined to be 1.5% in water through a comparative method using quinine sulfate as a reference.[29]

Silica nanoparticles modified chemically with terbium complexes (**Tb-SNPs**) were prepared by a modified microemulsion method[30] as follows. APTES (10 μL, 43 μmol) was added to a methanol solution (10 mL) of **EDTA-FSA-Tb complex** (44 mg, 59 μmol) and the resulting mixture was stirred for 1 h at room temperature. After the solvent was evaporated, TEOS (400 μL, 1.8 mmol) was added to the residue. The mixture was dissolved in a mixed solution of Triton X-100 (7.6 g), cyclohexane (23 g), 1-hexanol (5.9 g), and water (2.1 g). A sol-gel reaction[31] was initiated by adding 240 μL of 28% ammonia aqueous solution. The reaction was allowed to continue for 24 h at room temperature. After the reaction was finished by adding acetone, as-synthesized **Tb-SNPs** were washed by centrifugation with water several times in order to remove any surfactants and unreacted chemicals. The obtained nanoparticles were dispersed in water under vigorous ultrasonication. The quantum yield of covalently linked terbium complexes in silica nanoparticles was determined to be 11.7% in water by the same method as **EDTA-FSA-Tb complex**.

### Fluorescence imaging

**Tb-SNPs** for the fluorescence imaging were prepared by the above-mentioned synthetic method with an exception of the amount of APTES (20 μL, 85 μmol). Here, the amount of APTES was increased for the fluorescence enhancement. Before adding **Tb-SNPs,** COS-7 cells (originally isolated from African green monkey kidney) were seeded in Dulbecco's modified Eagle medium (Sigma) with 10% fetal bovine serum (Gibco BRL) on 35-mm glass bottom dishes (10,000 cells/well) and they were cultured at 37°C under 5% humidified $CO_2$ for two days. **Tb-SNPs** were introduced into the COS-7 cells by lipofectamine2000 (Life technologies), which is a cationic-lipid transfection reagent for cultured cell lines. A 3.0 μL of the aqueous solution containing **Tb-SNPs** was mixed with a 3.0 μL of the lipofectamine aqueous solution and it was voltexed vigorously. Then, the mixed solution was added directly into the culturing medium. After 24 h, the COS-7 cells were washed with PBS and their fluorescence images were captured by an IX71 epi-fluorescent microscopy (Olympus) equipped with a CCD camera (DP70, Olympus). **Tb-SNPs** were excited by a mercury lump through a 340-390-nm band-pass filter, and the emitted fluorescence was detected through a 420-nm long-pass filter.

## Results and discussion

### Synthesis

The synthesis of **EDTA-FSA-Tb complex** is shown in Scheme 1. An aqueous solution of EDTA was added to an aqueous solution of terbium acetate, and the resulting mixture was stirred for 1 h at 60°C. Then, an aqueous solution of FSA was added to the mixture, and the resulting mixture was stirred for 1 h at 60°C. The as-synthesized **EDTA-FSA-Tb complex** was purified by reprecipitation from water into warmed ethanol at 60°C. As **EDTA-FSA-Tb complex** has a reactive formyl group, it can be easily functionalized with an amino compound through a formation of a Schiff base.
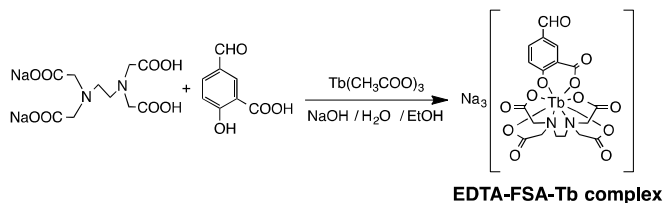
**Scheme 1**  Synthesis of **EDTA-FSA-Tb complex**.

For modifying silica nanoparticles chemically, **EDTA-FSA-Tb complex** was silylated by the reaction with APTES in methanol for 1 h at room temperature. As the Schiff base was obtained in high purity, the further purification was not necessary at this stage. In order to obtain **Tb-SNPs**, the silylated terbium complex was co-hydrolyzed of TEOS to form silica nanoparticles for 24 h at room temperature catalyzed by ammonium hydroxide in a water-in-oil emulsion using Triton X-100 as a surfactant in cyclohexane (Scheme 2). After the reaction was finished by adding acetone, the as-synthesized **Tb-SNPs** were isolated by repeated centrifugation and washing with water to remove any surfactants and unreacted chemicals. The obtained nanoparticles were finely dispersed in water. The concentration of **Tb-SNPs** was set at 1.0 wt % in the following experiments.
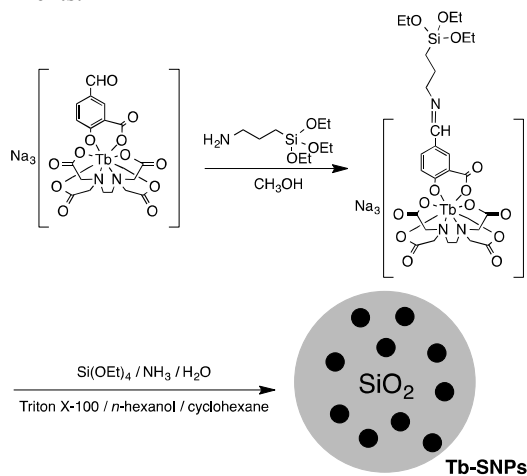
**Scheme 2**  Synthesis of **Tb-SNPs**.

### Characterization and property

The morphology and microstructure of **Tb-SNPs** were investigated by SEM measurements. Fig. 2a shows a typical SEM image, which demonstrated that **Tb-SNPs** were spherical and uniform in size (50 ± 5 nm in diameter). In addition, the size distribution of **Tb-SNPs** in water was obtained by DLS as shown Fig. 2b, and the average hydrodynamic diameter of **Tb-SNPs** was determined to 67 ± 14 nm. Although the hydrodynamic diameter determined by DLS was slightly larger than the real one determined from the SEM image, it was still thought that most of Tb-SNPs existed in water with high monodispersion. Also, the $\zeta$ potential of **Tb-SNPs** was measured as -46.8 ± 1.4 mV in water, indicating that the surface of **Tb-SNPs** was negatively charged like ordinary silica nanoparticles (ca. -50 mV).[32]
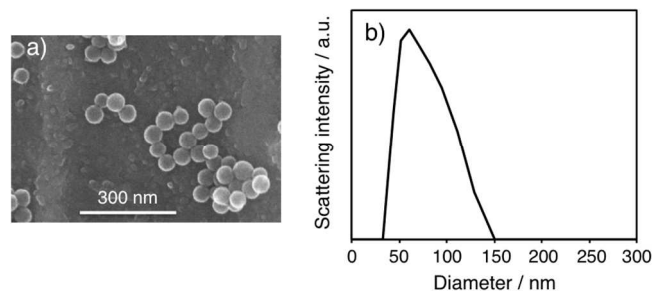
**Fig. 2**  (a) SEM image and (b) size distribution in water of **Tb-SNPs**.

The introduction amount of the terbium complex per one silica nanoparticle was investigated by the following method. Firstly, **Tb-SNPs** were completely dissolved in a mixed aqueous solution of HF and $HNO_3$. After the solvent was removed, the residue was diluted in a measuring flask. Then, the concentration of terbium ion was determined by ICP-MS. As a result, the introduction amount of terbium ion into silica nanoparticles was determined to 59 nmol $mg^{-1}$. This result means that $4.6 \times 10^3$ of terbium ions were introduced per one silica nanoparticle, in which the density of silica nanoparticles was assumed to be 1.96 g $cm^{-3}$.[30] This introduction amount is comparable with those of the same-sized polystyrene nanoparticles containing lanthanide chelates.[6]
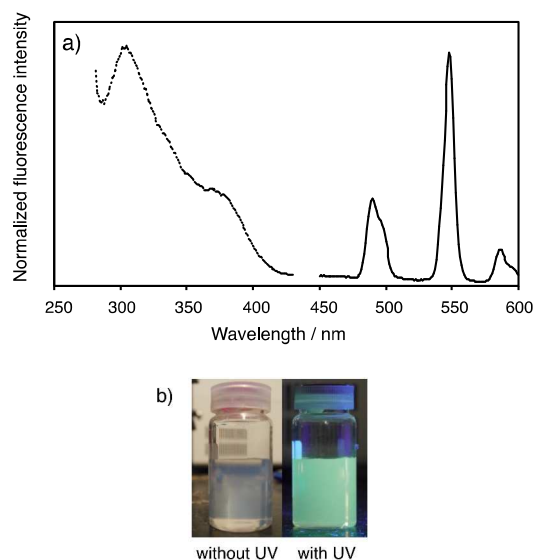
**Fig. 3**  (a) Excitation spectrum (dotted line) and emission spectrum (solid line) of **Tb-SNPs** in water. (b) Photographs of **Tb-SNPs** in water, taken with and without UV excitation.

Fig. 3a shows excitation and emission spectra of **Tb-SNPs** in water. The best excitation wavelength for the strongest fluorescent signal was 308 nm and the emission was monitored

at 548 nm. The emission spectrum of **Tb-SNPs** was very similar to that of **EDTA-FSA-Tb complex** regardless of excitation wavelength and its luminescent color was green (Fig. 3b). The sharp emission peaks at 490 nm, 546 nm and 585 nm are originated from electronic transitions in terbium from $^5D_4$ state to $^7F_6$, $^7F_5$ and $^7F_4$ state, respectively.[33] The quantum yield (11.7%) of **Tb-SNPs** in water was one-order higher than that (1.5%) of **EDTA-FSA-Tb complex** in water. This value of covalently linked terbium complexes in silica nanoparticles in water is comparatively high among reported aqueous terbium complexes.[34] Therefore, we can say that the fluorescence of **Tb-SNPs** is utilizable in water. As the control experiment, **Tb-SNPs** were also prepared from **EDTA-FSA-Tb complex** without APTES. In this case, the emission of terbium was not observed at all. Therefore, the formation of the Schiff base decisively contributes to the immobilization of terbium complexes into silica nanoparticles. The significance of the Schiff formation is also supported by the previous report,[35] where it was very difficult for lanthanide chelates to be encapsulated inside the silica network by physical adsorption due to the electrostatic repulsion. Furthermore, the introduction amount of terbium complexes into silica nanoparticles was controllable solely by changing the amount of APTES in the synthesis. Namely, the fluorescence intensity of **Tb-SNPs** was increased with an increase of the amount of APTES (Fig. S1). On the other hand, the increase of the APTES amount brought about the broadening of the size distribution in water (Fig. S2). Therefore, the ratio of terbium complexes to APTES should be optimized in forthcoming studies.

### Fluorescent stability

The fluorescent stability of **Tb-SNPs** was investigated. It is expected that the encapsulation of the terbium complex in silica nanoparticles minimizes the photodegradation.[16,36-38] Both aqueous solutions of dispersed **Tb-SNPs** and dissolved **EDTA-FSA-Tb-complexes** were prepared, and they were exposed to continuous UV irradiation in a fluorometer with a Xe lamp at 10 mW cm$^{-2}$. The fluorescence intensity at 548 nm was plotted against time course of the irradiation. Fig. 4a showed that the fluorescence of **Tb-SNPs** kept the intensity up to 60 min, whereas the fluorescence of free **EDTA-FSA-Tb complexes** declined. These results demonstrated that lanthanide chelates immobilized inside silica nanoparticles were protected from photobleaching. The interaction between silica and lanthanide chelates may play a significant role in the photostabilization.[39]

Next, the pH dependence on the fluorescence intensity of **Tb-SNPs** was also examined (Fig. 4b). The pH of solutions was adjusted using acetic acid and sodium hydroxide aqueous solution. In general, the lower fluorescence of lanthanide chelates is expected at the lower pH because of the dissociation of the terbium ion from the antenna ligand.[40] In the present case, the fluorescence of free **EDTA-FSA-Tb complexes** drastically decreased by lowering the pH. In contrast, the fluorescence of **Tb-SNPs** was almost constant in the pH range of 5-11 probably due to the fact that the antenna ligand locates near the terbium ion even under the acidic conditions because it is immobilized chemically into the silica matrix. Therefore, it was shown that the fluorescence of **Tb-SNPs** is applicable in the broad pH range of water.

To obtain further insights, fluorescence lifetimes were measured in both aqueous solutions of dispersed **Tb-SNPs** and dissolved **EDTA-FSA-Tb-complexes**. Fig. 5 shows decay curves at 548 nm upon excitation at 337 nm in semi-logarithmic scales with fitting curves. In Fig. 5a, a curve subtracted the slowest component is also plotted. In the case of **Tb-SNPs**, two components were observed after a spike response and the longer decay was predominant (Fig. 5a). The lifetime (1.5 ms) of **Tb-SNPs** was more than twice as long as that (0.68 ms) of free **EDTA-FSA-Tb complexes** (Fig. 5b), indicating that the terbium complex in silica nanoparticles is effectively protected form the quenching by water molecules. The shorter decay (0.45 ms) in the case of **Tb-SNPs** seems to be due to the fluorescence emitted from terbium complexes existing on the surface of silica nanoparticles because the lifetime was almost the same as that of free **EDTA-FSA-Tb complexes**, which means that the hydrophilic environments around the terbium complex are very similar between two cases. Probably, the slight decrease of the lifetime based on the introduction into SNPs may be originated from the existence of silanol groups around the terbium complex because the vibrational coupling of terbium ions with -OH oscillators results from silanol groups in addition to water molecules.[41] As a result, since the fluorescence lifetime of **Tb-SNPs** was much longer than that of conventional organic fluorescence compounds, **Tb-SNPs** are suitable for the emission label in such an aqueous solution containing organic impurities. This is because the fluorescence originated from organic compounds can be eliminated by time-resolved measurements.
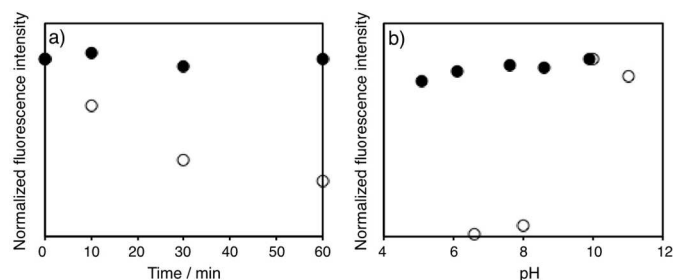


**Fig. 4** Fluorescence intensity changes at 548 nm of **Tb-SNPs** ( ● ) and **EDTA-FSA-Tb complex** (○) upon excitation at 308 nm in water (a) against time course under continuous UV irradiation and (b) with different pHs.
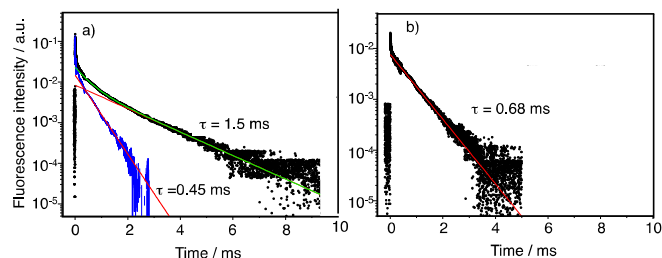


**Fig. 5** Decay curves at 548 nm of (a) **Tb-SNPs** and (b) **EDTA-FSA-Tb complex** upon excitation at 337 nm in water in semi-logarithmic scales with fitting curves. In (a), a curve subtracted the slowest component is also plotted.

### Colloidal stability

The colloidal stability of **Tb-SNPs** was evaluated by DLS under various aqueous conditions with different salt concentrations and pHs because the change of the salt concentration and pH can affect the surface charge of silica nanoparticles, which may induce the aggregation of **Tb-SNPs**. Fig. 6 shows the average diameter of **Tb-SNPs** in aqueous solution against time course after the addition of NaCl (150 mM) (Fig. 6a) and the pH change (Fig. 6b). Here, the average

diameters of **Tb-SNPs** were determined by their scattering intensity distributions. In the case of the salt addition, the average diameter slightly increased up to 100 min and saturated thereafter. Therefore, it was shown that the addition of 150 mM NaCl rarely affected the dispersibility of **Tb-SNPs**. On the other hand, the average diameter significantly increased under the acidic conditions (pH 4.3), indicating the slight aggregation. This is why the surface repulsion between silica nanoparticles is decreased due to the partial protonation of silanol groups. However, the precipitation of **Tb-SNPs** was not observed even under the acidic conditions. Also, the average diameter hardly changed under the basic conditions (pH 10.8) because almost all of silanol groups on the surface of silica nanoparticles deprotonates under the basic conditions. In conclusion of this section, we emphasize that the colloidal stability **Tb-SNPs** is very high under physiological aqueous conditions.
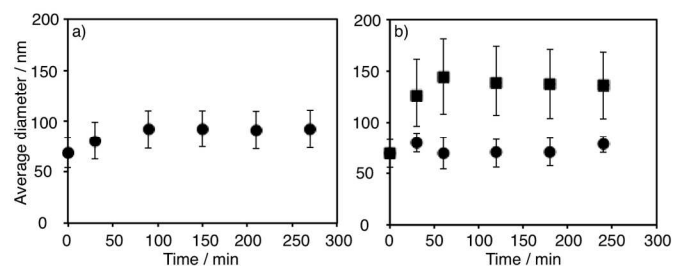


**Fig. 6** Time-course changes of average diameter of **Tb-SNPs** in aqueous solution (a) after addition of NaCl (150 mM;●) and (b) after pH change (pH 10.6;● and 4.3;■).

**Fluorescence imaging of COS-7 cells**
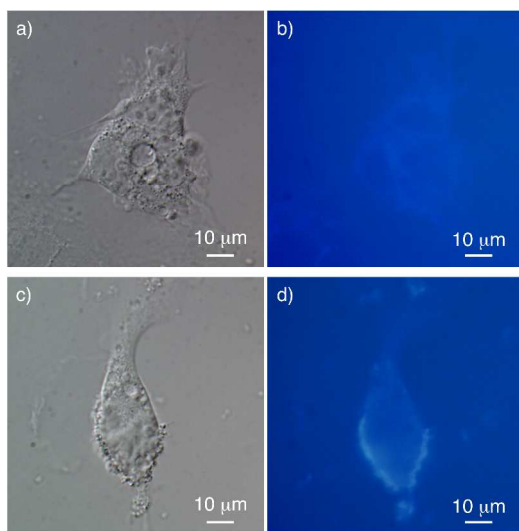


**Fig. 7** DIC images of COS-7 cells in the (a) absence and (c) presence of **Tb-SNPs**. (b) Fluorescent images of COS-7 cells in the (b) absence and (d) presence of **Tb-SNPs**.

To validate the possibility of **Tb-SNPs** as the fluorescent label, we attempted the fluorescence imaging of COS-7 cells using **Tb-SNPs**. To determine whether the fluorescence of **Tb-SNPs** can be observed in the cells, **Tb-SNPs** were introduced into the COS-7 cells using lipofectamine, which is a cationic-lipid transfection reagent for cultured cell lines, because **Tb-SNPs**, whose surface is negatively charged, can complex lipofectamine. Then the COS-7 cells were cultured in Dulbecco's modified Eagle medium with 10% fetal bovine serum at 37°C under 5% humidified $CO_2$ for 24 h. After washing the cells with PBS, the cell imaging was made using an epi-fluorescence microscopy. As the control experiment, the cell imaging in the absence of **Tb-SNPs** was also carried out. Fig. 7 shows the examples of the differential interference contrast (DIC) and fluorescent images of the COS-7 cells. The faint fluorescence observed in Fig. 7b was the autofluorescence originated from COS-7 cells because any fluorophore was not introduced into the cells in this case. As shown in Fig. 7d, the green fluorescence originated from **Tb-SNPs**, which was different from that observed in Fig. 7b, was observed in the cells containing **Tb-SNPs**. These results indicated that **Tb-SNPs** were successfully taken up into the cells and that they emitted the detectable fluorescence in the biological environment. However, the fluorescence intensity in the cells was considerably low. Probably, it is due to the low uptake efficiency of **Tb-SNPs** into the cells because it was shown in the previous section that **Tb-SNPs** emitted the fluorescence under physiological aqueous conditions. Taking into account the neutralized surface charge of **Tb-SNPs** complexed with lipofectamine, there was a possibility that **Tb-SNPs** aggregated before entering into the cells.

## Conclusions

In summary, we have demonstrated the efficient synthesis of fluorescent silica nanoparticles modified chemically with terbium complexes, and their fluorescent and colloidal properties in water. The photostability of terbium complexes was remarkably increased by the chemical immobilization into silica nanoparticles and most of fluorescent silica nanoparticles existed with high monodispersion under physiological aqueous conditions. Furthermore, their possibility as the fluorescent label for the cell imaging was tested. As a result, the green fluorescence originated from terbium complexes was observed in the cells and the fluorescent image was similar to the differential interference contrast image. According to our introduction method, however, only a small amount of fluorescent silica nanoparticles were introduced into the cells and they seemed to remain at the surface of the cells. Therefore, more works to improve the uptake efficiency without lipofectamine would be needed. For example, the introduction of folic acid molecules, which are well-known as targeting reagents for cancer cells,[42] into the surface of silica nanoparticles is desirable.[43] Further study on fluorescent silica nanoparticles modified chemically with lanthanide complexes such as europium and neodymium based on the synthetic scheme used in this study is also underway in our laboratory.

## Acknowledgements

## Notes and references

[a]*Department of Applied Chemistry, Faculty of Systems Engineering, Wakayama University, Sakae-dani 930, Wakayama 640-8510, Japan. E-mail: kkimura@center.wakayama-u.ac.jp; Tel: +81 73 457 8254*
[b]*Industrial Technology Center of Wakayama Prefecture, 60 Ogura, Wakayama 649-6261, Japan*

*<sup></sup>National Institute of Advanced Industrial Science and Technology, Central 6, 1-1-1 Higashi, Tsukuba 305-8566, Japan*

1   G. Mathis, *Clin. Chem.*, 1993, **39**, 1953-1959.
2   M. Xiao and P. R. Selvin, *J. Am. Chem. Soc.*, 2001, **123**, 7067-7073.
3   P. R. Selvin, *Annu. Rev. Biophys. Biomol. Struct.*, 2002, **31**, 275-302.
4   J. Feng, G. Shan, A. Maquieira, M. E. Koivunen, B. Guo, B. D. Hammok and I. M. Kennedy, *Anal. Chem.*, 2003, **75**, 5282-5286.
5   Z. Ye, M. Tan, G. Wang and J. Yuan, *Anal. Chem.*, 2004, **76**, 513-518.
6   P. Huhtinen, M. Kivelä, O. Kuronen, V. Hagren, H. Takalo, H. Tenhu, T. Lövgren and H. Härmä, *Anal. Chem.*, 2005, **77**, 2643-2648.
7   A. K. Saha, K. Kross, E. D. Kloszewski, D. A. Upson, J. L. Toner, R. A. Snow, C. D. V. Black and V. C. Desai, *J. Am. Chem. Soc.*, 1993, **115**, 11032-11033.
8   D. J. Posson, P. Ge, C. Miller, F. Bezanilla and P. R. Selvin, *Nature*, 2005, **436**, 848-851.
9   L.-L. Li, P. Ge, P. R. Selvin and Y. Lu, *Anal. Chem.*, 2012, **84**, 7852-7856.
10  S. Petoud, S. M. Cohen, J.-C. G. Bünzli and K. N. Raymond, *J. Am. Chem. Soc.*, 2003, **125**, 13324-13325.
11  P. G. Sammes and G. Yahioglu, *Nat. Prod. Rep.*, 1996, **13**, 1-28.
12  A. Beeby, I. M. Clarkson, R. S. Dickins, S. Faulkner, D. Parker, L. Royle, A. S. de Sousa, J. A. G. Williams and M. Woods, *J. Chem. Soc., Perkin Trans. 2*, 1999, 493-504.
13  S. Quici, G. Marzanni, M. Cavazzini, P. L. Anelli, M. Botta, E. Gianolio, G. Accorsi, N. Armaroli and F. Barigelletti, *Inorg. Chem.*, 2002, **41**, 2777-2784.
14  I. Hemmila and V. Laitala, *J. Fluoresc.*, 2005, **15**, 529-542.
15  T. Soukka, H. Harma, J. Paukkunen and T. Lovgren, *Anal. Chem.*, 2001, **73**, 2254-2260.
16  H. Zhang, Y. Xu, W. Yang and Q. Li, *Chem. Mater.*, 2007, **19**, 5875-5881.
17  Y. Chen, Y. Chi, H. Wen and Z. Lu, *Anal. Chem.*, 2007, **79**, 960-965.
18  A. P. Duarte, M. Gressier, M.-J. Menu, J. Dexpert-Ghys, J. M. A. Caiut and S. J. L. Ribeiro, *J. Phys. Chem. C*, 2012, **116**, 505-515.
19  M. C. Gomes, R. Fernandes, A. Cunha, J. P. Tome and T. Trindade, *J. Mater. Chem. B*, 2013, **1**, 5429-5435.
20  S. Bonacchi, D. Genovese, R. Juris, M. Montalti, L. Prodi, E. Rampazzo and N. Zaccheroni, *Angew. Chem., Int. Ed.*, 2011, **50**, 4056-4066.
21  G. Qian and M. Wang, *J. Am. Ceram. Soc.*, 2000, **83**, 703-708.
22  P. P. Lima, R. A. S. Ferreira, R. O. Freire, F. A. A. Paz, L. Fu, S. Alves, L. D. Carlos and O. L. Malta, *ChemPhysChem*, 2006, **7**, 735-746.
23  P. Lenaerts, A. Storms, J. Mullens, J. D'Haen, C. Görller-Walrand, K. Binnemans and K. Driesen, *Chem. Mater.*, 2005, **17**, 5194-5201.
24  L.-N. Sun, H.-J. Zhang, C.-Y. Peng, J.-B. Yu, Q.-G. Meng, L.-S. Fu, F.-Y. Liu and X.-M. Guo, *J. Phys. Chem. B*, 2006, **110**, 7249-7258.
25  E. DeOliveira, C. R. Neri, O. A. Serra and A. G. S. Prado, *Chem. Mater.*, 2007, **19**, 5437-5442.
26  G. Stork, A. Y. W. Leong and A. M. Touzin, *J. Org. Chem.*, 1976, **41**, 3491.
27  A. Natsch, H. Gfeller, T. Haupt and G. Brunner, *Chem. Res. Toxicol.*, 2012, **25**, 2203-2215.
28  M. Kanesato, Y. Kikkawa, E. Koyama and H. Tokuhisa, *Jpn. Kokai Tokkyo Koho*, 2009, JP2009292748.
29  J. H. Ahire, Q. Wang, P. R. Coxon, G. Malhotra, R. Brydson, R. Chen and Y. Chao, *ACS Appl. Mater. Interfaces*, 2012, **4**, 3285-3292.
30  S. Santra, P. Zhang, K. Wang, R. Tapec and W. Tan, *Anal. Chem.*, 2001, **73**, 4988-4993.
31  W. Stöber and A. Fink, *J. Colloid Interface Sci.*, 1968, **26**, 62-69.
32  T. Yu, A. Malugin and H. Ghandehari, *ACS Nano*, 2011, **5**, 5717-5728.
33  F. S. Richardson, *Chem. Rev.*, 1982, **82**, 541-552.
34  A. R. Mustafina, S. V. Fedorenko, O. D. Konovalova, A. Y. Menshikova, N. N. Shevchenko, S. E. Soloveva, A. I. Konovalov and I. S. Antipin, *Langmuir*, 2009, **25**, 3146-3151.
35  R. P. Bagwe, C. Yang, L. R. Hilliard and W. Tan, *Langmuir*, 2004, **20**, 8336-8342.
36  S.-W. Ha, C. E. Camalier, G. R. Beck Jr and J.-K. Lee, *Chem. Commun.*, 2009, 2881-2883.
37  W. Tan, K. Wang, X. He, X. J. Zhao, T. Drake, L. Wang and R. P. Bagwe, *Med. Res. Rev.*, 2004, **24**, 621-638.
38  H. Ow, D. R. Larson, M. Srivastava, B. A. Baird, W. W. Webb and U. Wiesner, *Nano Lett.*, 2005, **5**, 113-117.
39  Q. Xu, L. Li, B. Li, J. Yu and R. Xu, *Microporous Mesoporous Mater.*, 2000, **38**, 351-358.
40  J. Hovinen and P. M. Guy, *Bioconjugate Chem.*, 2009, **20**, 404-421.
41  C. Tiseanu, M. U. Kumke, V. I. Parvulescu, A. Gessner, B. C. Gagea and J. A. Martens, *J. Phys. Chem. B*, 2006, **110**, 25707-25715.
42  J. F. Kukowska-Latallo, K. A. Candido, Z. Y. Cao, S. S. Nigavekar, I. J. Majoros, T. P. Thomas, L. P. Balogh, M. K. Khan and J. R. Baker Jr., *Cancer Res.*, 2005, **65**, 5317-5324.
43  M. Tagaya, T. Ikoma, T. Yoshioka, Z. Xua and J. Tanaka, *Chem. Commun.*, 2011, **47**, 8430-8432.